

Article

The Effect of Lubricant's Viscosity on Reducing the Frictional-Induced Fluctuation on the Onset of Friction

Shutian Liu ¹, Juncheng Lv ^{1,2} and Chuanbo Liu ^{1,*}

¹ School of Mechanical and Electronic Engineering, Wuhan University of Technology, Wuhan 430070, China; shutian_liz@whut.edu.cn (S.L.); juncheng.lv@sgmw.com.cn (J.L.)

² Shanghai General Motors Wuling, Liuzhou 545027, China

* Correspondence: lchb72@whut.edu.cn

Abstract: The initial friction stage between the contacting materials would generate a maximum shear force and an unstable fluctuating time, which had a negative effect on the entire frictional system, especially at low temperature conditions. In order to decrease the occurring shear force and fluctuating time on the onset of friction, two different lubricating oils were applied in this study to investigate the influence of lubricant's viscosity on these friction behaviors. The frictional experiments were conducted between the steel ball and the 40CrMnMo, and special attention was paid to the relationship between maximum friction force, fluctuating time, frictional vibration and the initial lubricant temperature. The results showed that the friction force first increased to the maximum value and then experienced an oscillation damping period (fluctuating time) before it reached a stable state. And this fluctuating behavior caused corresponding vibrations on the initial contacting. However, compared to the high viscosity lubricating oil (HO), the low viscosity lubricating oil (LO) contributed to more than 50% reductions on max friction force, fluctuating time and vibration at the cold start (0 °C). Moreover, the weakened initial frictional fluctuation was conducive to generating a low and stable friction coefficient (COF) and wear loss of the long-term test. The discrepancy on lubricating performance was that the low viscosity provided high fluidity, which allowed rapid distribution of the lubricant between the contacting surfaces and formed an intact lubricating film. Similarly, the high temperature decreased the viscosity of HO and thus led to satisfactory friction reductions. The knowledge gained herein provides a supporting theory on the design and preparation of a lubricating oil with high performance.



Citation: Liu, S.; Lv, J.; Liu, C. The Effect of Lubricant's Viscosity on Reducing the Frictional-Induced Fluctuation on the Onset of Friction. *Lubricants* **2024**, *12*, 136. <https://doi.org/10.3390/lubricants12040136>

Received: 25 March 2024

Revised: 12 April 2024

Accepted: 14 April 2024

Published: 17 April 2024



Copyright: © 2024 by the authors. Licensee MDPI, Basel, Switzerland. This article is an open access article distributed under the terms and conditions of the Creative Commons Attribution (CC BY) license (<https://creativecommons.org/licenses/by/4.0/>).

Keywords: friction fluctuations; friction vibration; onset of friction; lubricant viscosity; cold start

1. Introduction

The development of more precise instruments had demanded the establishment of working conditions that were both smoother and more stable. This had led to a reduction in the levels of vibration, noise, and energy loss [1–4]. The friction-induced behavior that was generated between the contacting surfaces was the primary factor that determined the instrument's fluctuating performance when it was functioning. The deformation of the surface that occurred during contact would lead to variations in the force of friction, as well as vibrations and noise that were created by friction, which would ultimately lead to a decrease in stability [5–9]. As a consequence of this, a wide variety of high-performance lubricants, which were either derived from petroleum or that were obtained from biological sources, have been utilized widely for the goal of reducing surface deformations [10–12].

Lubricants were able to give satisfactory lubricating performance on the stable stage of mechanical equipment. Nevertheless, boundary lubrication and even poor lubrication usually occurred during start-up, deceleration, and direction-changing situations [13–15]. This was the case even though lubricants were able to provide satisfactory lubricating performance there. For instance, the water-lubricated stern bearing experienced audible

and visible vibrations and noises during the beginning of the operation and when the ship was changing directions [16–20]. While the sliding process was taking place, the production of a lubricating film between the contact surfaces did not take place immediately during the initial phase. Rather, it took place gradually over the course of the process. Due to the lack of an unsatisfactory lubricating condition, the frictional pairs came into close contact with one another, which ultimately led to the development of severe frictional behaviors.

Additionally, it was noticed that the lubricating capabilities of the lubricants were directly influenced by the temperature at which the working environment was being maintained. A time frame of 10 s following the cold start of a vehicle engine was observed to be responsible for around seventy percent of the wear characteristics discovered. The reason for this was that lubricating oil has a limited capacity to flow smoothly at low temperatures, which causes it to spread unevenly and quickly across the surfaces that are in contact with it. As a consequence of this, boundary lubrication and direct contact of materials took place [21–23]. In addition, it was hypothesized that the deformations that emerged during the beginning of the frictional process would become more pronounced with subsequent friction, which would ultimately result in unstable fluctuations. Consequently, in an effort to improve the fluidity of lubricants, a greater emphasis had been made on the creation and formulation of lubricating oils that were characterized by low viscosity.

The transmission bearings were necessary to reduce the running-in period of lubrication due to the motor's progressively higher speed output [24–27]. In this scenario, the progressive implementation of low viscosity lubricating oils in electric drive cars had been undertaken with the aim of mitigating energy loss and enhancing energy efficiency. Nevertheless, there has been a lack of comprehensive research undertaken on the impact of lubricant viscosity on the early frictional behaviors observed during contact. Hence, this study selected two lubricating oils with varying viscosities to evaluate their lubricating capabilities during the initiation of friction. A significant emphasis was placed on the maximum friction force and the duration of fluctuation as well as the frictional vibration. Furthermore, the research involved conducting long-term friction studies to uncover the impact of the initial frictional behaviors on the overall friction state. The findings obtained in this study were advantageous for the development and production of lubricating oil with low viscosity, resulting in a significant decrease in frictional fluctuations.

2. Methods and Experiments

2.1. Preparations of the Lubricants with Different Viscosity and the Friction Tests

Two types of lubricating oils were investigated in this study, which named high-viscosity lubricating oil (HO) and low-viscosity lubricating oil (LO). Both of these oils were poly (ethylene glycol) α Alkene base oils, but their viscosities were different owing to the design of different length molecular chains, shown in Figure 1A,B. These lubricating oils were supplied by the Guangxi New Energy Vehicle Laboratory. The selection of carbon steel and 40CrMnMo as frictional pairings on the basis of their broad utilization as materials for bearings and drive shafts in a variety of engineering applications. In order to conduct all of the frictional testing, the R-tec tribo-tester (Rtec Instruments Inc., San Jose, CA, USA) and ball-plate reciprocating frictional tests (Figure 1C,D) were utilized. In the process of the friction test, the carbon steel ball, with a diameter of 10 mm, was kept in a stationary position at the top, while the bottom 40CrMnMo plate went through a reciprocating motion powered by a motor. In addition, the reciprocating model was utilized because of its capacity to reproduce a rapid sliding movement that begins from a stationary state in a manner that was repeated frequently. Furthermore, in order to ensure that the steel ball and the 40CrMnMo plate had a smooth surface, they were subjected to a polishing process to achieve an S_a value of $0.004 \mu\text{m}$ prior to the implementation of the testing procedure. Moreover, the vibration sensor was fixed on the upper fixture for collecting the acceleration data along the sliding direction.

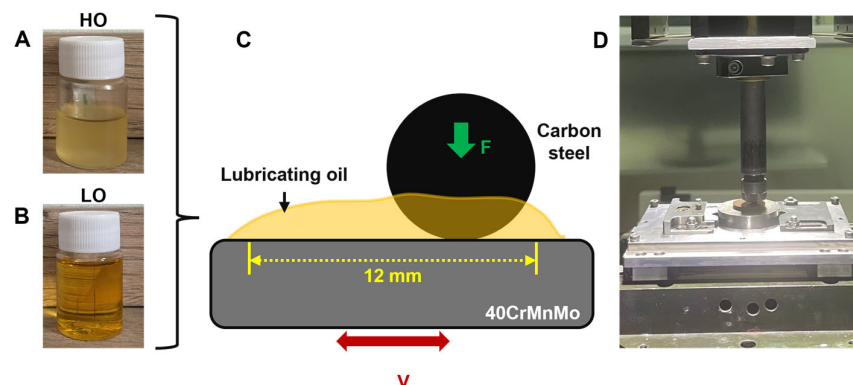


Figure 1. Lubricants and frictional experiments: the high viscosity (HO) (A) and low viscosity (LO) (B) lubricating oils and the ball–plate reciprocating friction model (C,D) were used.

The carbon steel ball and the 40CrMnMo were submerged in the lubricating oils in order to guarantee an adequate amount of lubricant between the surfaces. The sliding frequencies were set to 0.1, 0.5, 1, 2, and 5 Hz, and the loads were set to 10, 15, 20, 25, and 30 N in order to study the varying lubricating performances of the individual components under a variety of test situations. When conducting each new friction test, a new carbon steel ball, 40CrMnMo plate, and lubricant were utilized. In addition, all data from the tests was taken at intervals of 0.0001 s. For the purpose of ensuring that the results were consistent, each test was carried out three times. In addition, the HO and LO lubricating oils were placed in water baths at 0 °C and 100 °C individually for 2 h to ensure that different lubricant temperatures were achieved. And the limitation of 100 °C was selected to avoid the decline of lubricating oil performance in high-temperature environments.

2.2. Measurement Techniques and Equipment

The rheometer (Netzsch Kinexus Lab+, Netzsch, Germany) had been used to test the rheological properties of the HO and LO lubricants under different shear rates and temperatures. The deforming behaviors of the frictional pairs were observed by using the confocal laser scanning microscopy (CLSM) (VX-X1000, Keyence, Osaka, Japan) and the scanning electron microscope (SEM) (VEGA3, Tescan, Brno, Czech Republic). The vibration behavior on the onset of friction was detected by using a vibration sensor (4535-B, Bruel & Kjaer, Naerum, Denmark).

3. Results and Discussion

3.1. Rheological Properties of the HO and LO with the Temperatures and Shear Rates

Figure 2 illustrated the rheological properties of the HO and LO lubricating oils at the increasing temperatures and shear rates. At a temperature of 0 °C, the viscosities of the HO and LO were 2055 and 146 mPa s, respectively. In contrast, the viscosity of the HO fell dramatically as the temperature increased, and it stayed stable at 153 mPa s throughout the experiment (Figure 2A). Based on this result, it was claimed that the HO exhibited temperature sensitivity and the ability to demonstrate improved fluidity when subjected to higher temperatures. On the other hand, a decrease in margin was found on the LO, with a value of 94 mPa s being observed when temperatures were raised. In addition, the viscosities of the HO and LO remained relatively unchanged as the shear rate increased, with average values of 487 and 54 mPa s, respectively, at a temperature of 23 °C (Figure 2B). According to the findings of the rheological analysis, the viscosity of the HO at low temperatures was significantly high. This led to a reduction in fluidity, which in turn hindered the creation of a lubricating film, particularly at low temperatures.

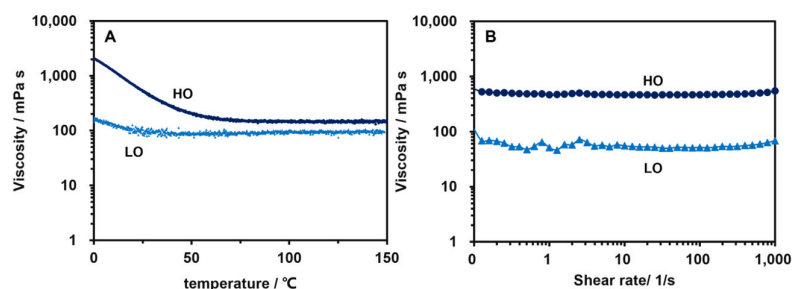


Figure 2. Rheology properties of the HO and LO lubricants under the increasing temperatures (A) and shear rates (B).

3.2. The Friction Fluctuations Generated on the Onset of Friction under Different Lubricants

A presentation of the results of the frictional behaviors that were acquired under the HO and LO lubrications is displayed in Figure 3. Both 0 and 100 °C were used as the lubricant temperatures for the tests, and the testing period was the initial 0.6 s. Due to insufficient lubrication, the friction pairs were in a state of boundary lubrication during the beginning stages of the friction process, which led to an excessive shear force. Nevertheless, the shear force decreased at a quick rate as the lubricant spread and a lubricating layer formed [28–30]. The friction force that was identified would initially attain its highest value, which is referred to as the maximum friction force. At a temperature of 0 °C, the max force value was measured at 4.2 N of the HO, but the LO brought it down to 3.3 N (Figure 3A,B). In addition, the maximum friction force went through a phase of exponential decline and then eventually arrived at a steady state, which was referred to as the fluctuating time. Calculating the derivative of the friction force curve with respect to time was utilized to ascertain the quantification of this variable duration. And the time it took for the friction force to reach stability was named the fluctuation time. The HO exhibited a fluctuation time of 0.3 s, which was almost three times bigger than that of the LO's value (0.098 s) (Figure 3A,B black line). Because of the low viscosity of the lubrication oil (LO), it was able to disseminate evenly over the surfaces that were in touch with it and rapidly offer a lubricating action even when the temperature was low. This was attributed to the observed decrease in fluctuation time. There was, however, a restriction placed on the fluidity of the HO because of its extraordinarily high viscosity at low temperature, which indicated that the creation of a lubricating layer required a longer period of time. As a consequence of this, the long fluctuation time was observed.

The viscosities of the HO and LO showed decreasing trends with the increasing temperatures, which indicated the improvement in fluidity (Figure 2). In this case, the maximum friction forces, at 100 °C, decreased from 3.3 N to the 2.8 N of the LO as well as from 4.2 N to the 2.9 N of the HO (Figure 3(A-1,B-1)). Similarly, the improved fluidity, at high temperatures, of the lubricant reduced the time of spreading and film generation, which contributed to around 30% reductions in the fluctuation time of the HO (declined from 0.3 s to the 0.2 s). However, the margin decrease was performed on the LO's fluctuation time at a high temperature which could be attributed to the viscosity characteristics that did not differ significantly between high and low temperatures. Despite a decrease of about 30% compared to the cold start, the HO caused a fluctuation duration of 0.2 s, which was approximately twice as long as the LO at 100 °C (0.09 s in Figure 4B). The lower fluidity of the HO at 100 °C (147.1 mPa s) compared to the LO (93.4 mPa s) could be attributed to its high viscosity. As a result, the HO required a longer time to disperse the lubricant and formed a film. Consequently, a greater degree of fluctuating time than the LO was observed.

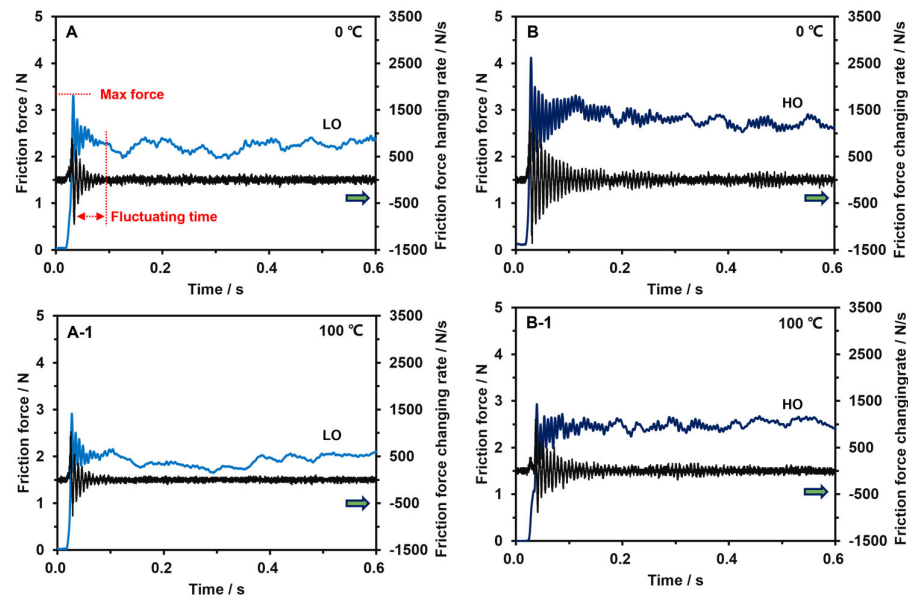


Figure 3. The initial fluctuation of friction under different starting temperatures at 0.1 Hz and 20 N: the LO (A) and HO (B) at 0 °C, and the LO (A-1) and HO (B-1) at 100 °C.

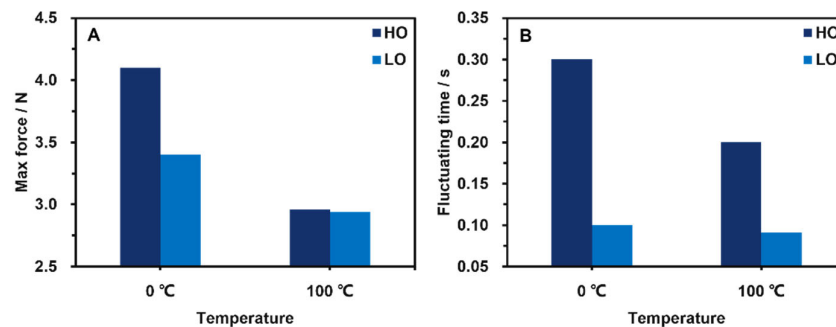


Figure 4. The initial max friction force (A) and fluctuating time (B) of LO and HO lubricants under 0 °C and 100 °C.

3.3. The Friction-Induced Vibrations on the Onset of Friction under Different Lubricants

Figure 5 exhibited the vibrations caused by friction at the onset of friction in the 40CrMnMo sample when subjected to HO and LO lubrications at two temperatures of 0 and 100 °C. The occurrence of vibrating behaviors was detected during the initial period, potentially indicating the presence of friction variations, as depicted in Figure 3. Due to the limited fluidity of the HO lubricating oil, the lubricating performance failed to provide the expected lubricating effect on the initiation of friction, resulting in the generation of a maximum friction force and prolonged fluctuation time. Consequently, this led to the manifestation of vibrating behaviors, ranging from -3.8 to 3.7 m/s^2 , which persisted for a duration of 0.2 s (Figure 5B). Nevertheless, the vibrating behaviors shown by the LO varied between -3.1 and 2.4 m/s^2 and had a duration of 0.05 s due to its low viscosity, as depicted in Figure 5A. Figure 5(A-1,B-1) showed the vibratory characteristics of the LO and HO at a temperature of 100 °C, which performed noticeable reductions compared to their values at low temperatures. During a period of 0.06 s, the HO experienced a vibration range of -2.1 to 1.9 m/s^2 , whereas the LO resulted in a vibration range of -1.3 to 1.5 m/s^2 during a period of 0.03 s. The observed phenomenon can be attributed to the positive correlation between temperature and the fluidity of HO and LO lubricants. This increase in temperature led to an increased production rate of the lubricating film, resulting in a rapid improvement in lubrication performance. Furthermore, it could be demonstrated that

the fluctuation in friction caused by the initial friction were responsible for the associated vibration characteristics.

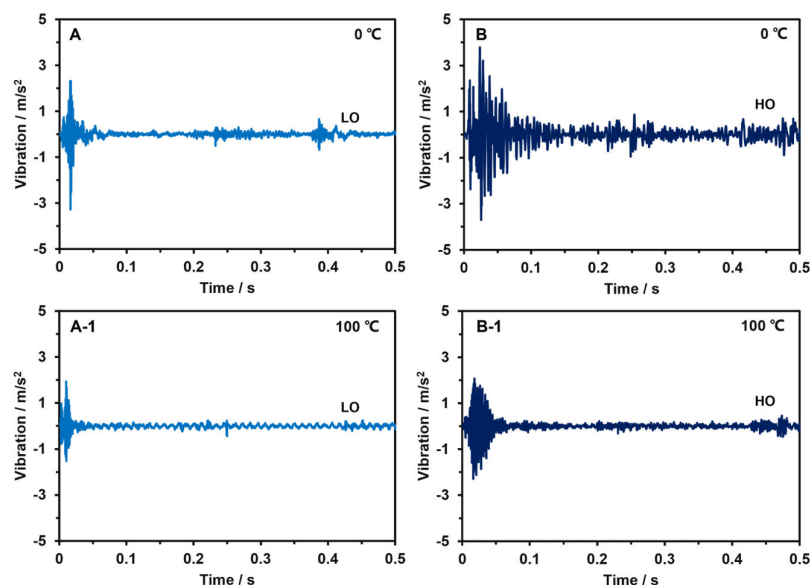


Figure 5. The frictional-induced vibrations under different starting temperatures at 0.1 Hz and 20 N: the LO (A) and HO (B) at 0 °C and the LO (A-1) and HO (B-1) at 100 °C.

3.4. Coefficient of Friction Responses of the HO and LO under the Long-Term Friction

The different frictional performances on the onset of friction under the HO and LO lubricants would influence their subsequent long-term tribological properties. Therefore, Figure 6 displayed the COF responses of the 40CrMnMo and steel ball under 1800 s long-term friction at different sliding frequencies and applied loads. In addition, the initial temperature of each lubricant was maintained at 0 °C, and no temperature adjustments were made during the friction process. The COF curve of the HO, at a low load (10 N), exhibited a significant increased trend from the initial value at 0.09 to the maximum value at 0.105, which was followed by a reduction as the friction proceeded (Figure 6A). At the initial friction, the HO with poor low-temperature fluidity could not provide good lubrication performance, thus increasing the COF. However, the lubricant gradually distributed evenly and formed a lubricating film as friction progressed which led to the decrease in COF. Similarly, the COF curve of the HO performed a noticeable increase in the running-in period at the high applied load (25 N), but the increased contact area between the frictional pairs caused higher friction coefficient values under high loads. Therefore, the maximum value climbed to around 0.12 (Figure 6B). Conversely, owing to the fact that the LO lubricating oil weakened the frictional behaviors on the onset of friction, which therewith maintained the COF curves at a low and stable value (around 0.09) for both low and high applied loads (10 N and 25 N, respectively). The observed phenomenon could potentially be attributed to the low viscosity property of LO, which conferred exceptional liquid fluidity and facilitated rapid dispersion over the surfaces in contact. Consequently, the initiation of friction resulted in the formation of low and consistent frictional behaviors, as demonstrated in Figures 3 and 4. This, in turn, led to the development of a stable COF curve with a low value. In contrast, the occurrence of fluctuating COF curves was observed in the HO lubrication due to the high maximum friction force, prolonged fluctuation time, and noticeable deformations. Furthermore, the limited fluidity of HO lubricant hindered its ability to effectively distribute itself throughout the surfaces in contact, particularly under high applied loads. Consequently, a clear upward trend was generated, leading to the attainment of a high COF value.

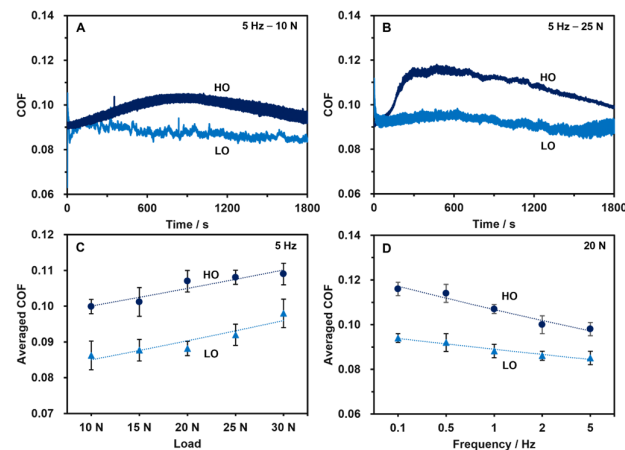


Figure 6. The coefficient of friction (COF) responses of the LO and HO lubricants under long-term friction at various testing conditions: the COF curves under 10 N (A) and 25 N (B) and their averaged COFs with loads (C) and frequencies (D).

Figure 6C shows the averaged COF responses of the HO and LO lubricants with the increasing applied loads. Both lubricants exhibited exceptional load-bearing characteristics, with a slight upward trend observed as the applied load increased. The LO increased the value from 0.086 at a load of 10 N to 0.095 at a load of 30 N, whereas the HO increased from 0.101 at a load of 10 N to 0.109 at a load of 30 N. The averaged COF with a margin increases in load proved that the HO and LO exhibited satisfactory pressure performances. In addition, the COF responses of the LO exhibited a reduced reliance on the escalating sliding frequencies, as evidenced by its smaller decline slope compared to the HO lubricant (Figure 6D). Specifically, the averaged COF decreased from 0.118 at 0.1 Hz to the 0.102 at 5 Hz of the HO while a slight reduction from 0.093 to 0.087 (increased from 0.1 to 5 Hz).

3.5. Surface Morphologies of Specimens after the HO and LO Lubrications

Figure 7 depicted the surface topographies of the 42CrMnMo surfaces that were treated under HO and LO lubricating conditions. The worn scratch and its three-dimensional shape of the HO lubrication were displayed in Figure 7A,B, and it was noticed that the worn scratch had a significant depth and width. It was evident from Figure 7C,D that the utilization of the LO led to a substantial reduction of more than 20% in the depth of wear. Specifically, the depth of wear decreased from 5.8 μm when lubricated with HO to 4.3 μm when the LO was applied. Figure 7E demonstrated that the LO yielded a smaller worn width value of 1322 μm compared to the HO value of 1395 μm .

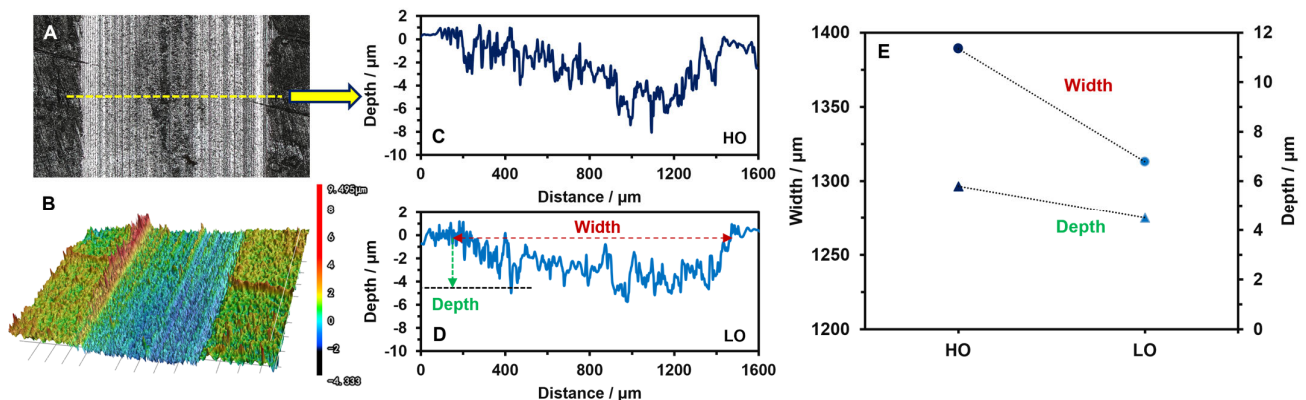


Figure 7. Surface topographies of the tested specimens at 5 Hz, 20 N, and 1800 s: the worn scratch (A) and its 3D topography (B) of the HO lubricant; scratching curves of the HO (C) and LO (D) and their depth and width comparing (E).

Additionally, the wear volume could be calculated by applying the integral principle on the measured cross-section curves. V represented the wear volume, and it was determined by the wear distance L , worn width W , unit increment length (unit testing interval) Δx , and the wear depth of the i th rectangle ($f(x_i)$). With Δx of 0.001 mm in the testing interval, any area (S_{ai}) of the unit rectangle could be calculated by

$$S_{ai} = f(x_i)\Delta x$$

And the full cross section of the wear scratch thus had an area of

$$S_{all} = \sum_{i=1}^{W/\Delta x} S_{ai}$$

Therefore, the whole wear volume could be calculated as follows:

$$V = S_{all} \times L = L \times \sum_{i=1}^{W/\Delta x} f(x_i)\Delta x$$

The wear volume results were computed, revealing a reduction of approximately 27% in the volume of 0.022 mm³ for the LO lubrication compared to 0.031 mm³ for the HO lubrication. The analysis of wear depth and volume data revealed that the LO lubricant exhibited superior performance in terms of reducing the worn loss. This was attributed to the LO providing a satisfactory lubricating performance in the initial stage of wear, thereby reducing the deforming behavior on the sample surface during contact, and as a result, the weakened wear loss was observed after a continuous wear process.

3.6. Micro Morphologies of the Specimen after the HO and LO Lubrications

In Figure 8, the surface morphologies of the 40CrMnMo material were depicted under the influence of the HO and LO lubricants, and specifically, attention was paid to the worn morphologies on the initial process. Owing to the reciprocating model being reproduced as a rapid sliding movement that begins from a stationary state frequently, the wear morphology at the first location could be regarded as the result of numerous start-up frictions. Figure 8A shows that the noticeable cracks and grooves occurred on the worn surface with the HO lubricating oil. The low fluidity of the HO limited the spread of the lubricant around the contacting interfaces at the onset of friction, and the poor or boundary lubricating conditions caused direct contact of the frictional pairs. Under the effect of shear force and applied load, the deformations were generated and were exacerbated by the frictional effects. As a result, the higher worn depth at the initial location was observed at 3.2 μm (Figure 8(A-1)). However, because of the high fluidity of LO, which conferred lubrication capabilities for the purpose of smoothing the deformed surface, the rapid creation of a lubricating layer during the initial contact period was made possible. Therefore, the application of the LO lubricating oil led to the almost smooth worn surface with tiny grooves and contributed to a worn depth of less than 2.1 μm (Figure 8(B,B-1)).

Figure 9 depicted the micro-morphologies on the worn surfaces of 42CrMnMo following the application of HO and LO lubricants. The worn surface exhibited visible cracks when lubricated with HO, whereas the worn surface with LO showed only minor deformations (Figure 9A,B). The presence of a smooth worn surface in the LO lubrication system had been found to contribute to a stable friction process, as seen by the stable COF curve depicted in Figure 6A,B. Due to its limited fluidity, the HO lubricant exhibited inadequate diffusion and failed to establish a uniform lubricating layer at contact initiation, resulting in suboptimal and limited lubrication conditions. The surfaces that came into direct contact would undergo deformation due to the cutting force and vertical load, as seen in Figures 8 and 9. As the friction behavior proceeds, the lubricating film gradually spread and established by the HO, and the reduction in the friction process was observed. However, following repeated contact, the existing deformations finally became severe

and apparent (Figure 9(A,A-1,A-2)). In contrast, the LO lubricant exhibited negligible deformation and fluctuation characteristics upon the initiation of friction, hence assuring its stability throughout extended periods.

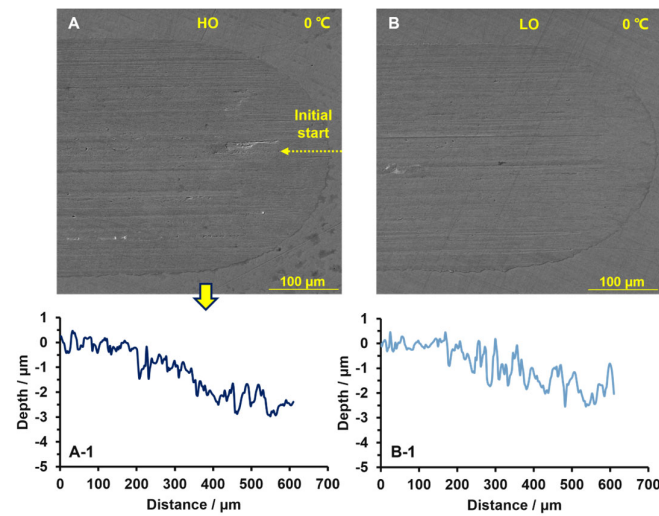


Figure 8. Surface morphologies of the tested specimens on the onset of friction at 0.1 Hz, 20 N, and 0 °C: micro-morphology (A) and scratching curve (A-1) of the HO and the micro-morphology (B) and scratching curve (B-1) of the LO.

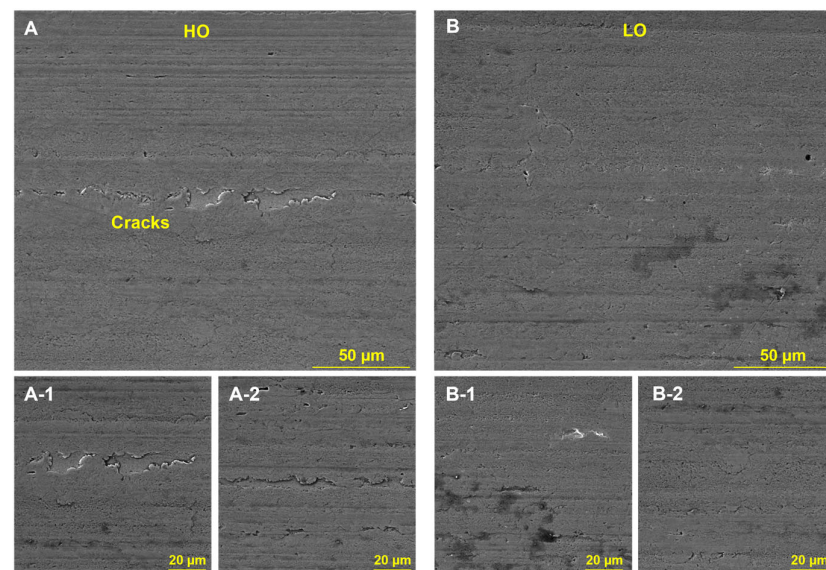


Figure 9. Micro surface morphologies of the tested specimens under the HO (A) and LO (B) lubrications as well as their detailed worn deformation (A-1), (A-2) and (B-1), (B-2) individually.

4. Conclusions

This study employed two distinct lubricating oils with different viscosities to examine the impact of viscosity on the mitigation of friction variations during the initiation of friction. Due to the low viscosity and high fluidity of LO, it could quickly spread throughout the surfaces, resulting in the formation of a complete lubricating film for reducing friction. The experimental findings indicated that there were reductions of over 50% in the first maximum friction force, fluctuation time, and friction vibration as compared to the HO under cold start conditions (0 °C). In this scenario, the quick formation of a lubricating film on the surface that made contact was advantageous for producing consistent friction characteristics over an extended period of time. This was demonstrated by a low coefficient

of friction (COF) value and minimal wear loss. The information acquired in this study was valuable in the development of a novel lubricant that exhibits efficient performance in mitigating initial friction variations.

Author Contributions: S.L.: Conceptualization, Methodology, Data Curation, Writing—Original Draft, Visualization. J.L.: Project administration, Conceptualization, Resources. C.L.: Supervision, Project administration, Methodology, Writing—Review and Editing. All authors have read and agreed to the published version of the manuscript.

Funding: This paper is supported by the Guangxi Science and Technology Major Program (Guangxi New Energy Vehicle Laboratory Special Project: AA23062066).

Data Availability Statement: The original contributions presented in the study are included in the article, further inquiries can be directed to the corresponding author.

Acknowledgments: The Tribology Laboratory of Marine Engineering of the Wuhan University of Technology is acknowledged for tribological equipment.

Conflicts of Interest: Juncheng Lv was employed by Shanghai General Motors Wuling. The remaining authors declare that the research was conducted in the absence of any commercial or financial relationships that could be construed as a potential conflict of interest.

References

1. Tang, D.X.; Xiao, K.; Xiang, G.; Cai, J.L.; Fillon, M.; Wang, D.F.; Su, Z.L. On the nonlinear time-varying mixed lubrication for coupled spiral microgroove water-lubricated bearings with mass conservation cavitation. *Tribol. Int.* **2024**, *193*, 109381. [[CrossRef](#)]
2. Liu, D.; Zhou, L.; Zhang, D.; Wang, H. A strategy of vibration control for rotors with dry friction dampers. *J. Vib. Control* **2023**, *29*, 2907–2920. [[CrossRef](#)]
3. Jin, Y.; Liu, Z.L.; Zhou, X.C. Theoretical, numerical, and experimental studies on friction vibration of marine water-lubricated bearing coupled with lateral vibration. *J. Mar. Sci. Technol.* **2020**, *25*, 298–311. [[CrossRef](#)]
4. Zhang, Z.; Ouyang, W.; Liang, X.X.; Yan, X.P.; Yuan, C.Q.; Zhou, X.C.; Guo, Z.W.; Dong, C.L.; Liu, Z.L.; Jin, Y.; et al. Review of the evolution and prevention of friction, wear, and noise for water-lubricated bearings used in ships. *Friction* **2024**, *12*, 1–38. [[CrossRef](#)]
5. Tiwari, S.K.; Kumaraswamidhas, L.A. The Effect of Friction Induced Noise, Vibration, Wear and Acoustical Behavior on Rough Surface: A Review on Industrial Perspective. In *Advances in Engine Tribology*; Springer: Singapore, 2021; pp. 153–165. [[CrossRef](#)]
6. Abdulbasit, A.H.; Shawnam, R.J. A review on manufacturing the polymer composites by friction stir processing. *Eur. Polym. J.* **2022**, *178*, 111495.
7. Wang, Y.S.; Guo, H.; Yuan, T.; Ma, L.F.; Liu, N.N.; Sun, P. Friction-induced noise of vehicle wiper-windshield system: A review. *Results Eng.* **2023**, *20*, 101557. [[CrossRef](#)]
8. Lontin, K.; Khan, M. Interdependence of friction, wear, and noise: A review. *Friction* **2021**, *9*, 1319–1345. [[CrossRef](#)]
9. Qin, H.L.; Yang, C.; Zhu, H.F.; Li, X.F.; Li, Z.X.; Xu, X. Experimental analysis on friction-induced vibration of water-lubricated bearings in a submarine propulsion system. *Ocean Eng.* **2020**, *203*, 107239.
10. Hyholm, N.; Espallargas, N. Functionalized carbon nanostructures as lubricant additives—A review. *Carbon* **2023**, *201*, 1200–1228.
11. Zhao, X.Y.; Li, D.Q.; Zhu, H.M.; Ma, J.Y.; An, Y.X. Advanced developments in environmentally friendly lubricants for water-based drilling fluid: A review. *RSC Adv.* **2022**, *12*, 22853–22868. [[CrossRef](#)]
12. Malik, M.A.I.; Kalam, M.A.; Mujtaba, M.A.; Almomani, F. A review of recent advances in the synthesis of environmentally friendly, sustainable, and nontoxic bio-lubricants: Recommendations for the future implementations. *Environ. Technol. Innov.* **2023**, *32*, 103366. [[CrossRef](#)]
13. Nathalia, D.S.A.S.; Vinicius, R.R.; Marco Tulio, C.F. Review of engine journal bearing tribology in start-stop applications. *Eng. Fail. Anal.* **2020**, *108*, 104344.
14. Fayaz, A.M.; Noor, Z.K.; Arshad, N.S.; Saad, P. Friction based solid state welding—A review. *Mater. Today Proc.* **2022**, *62 Pt 1*, 55–62.
15. Lee, P.; Zhmud, B. Low Friction Powertrains: Current Advances in Lubricants and Coatings. *Lubricants* **2021**, *9*, 74. [[CrossRef](#)]
16. Xie, Z.L.; Jiao, J.; Yang, K.; Zhang, H. A state-of-art review on the water-lubricated bearing. *Tribol. Int.* **2023**, *180*, 108276. [[CrossRef](#)]
17. Wang, H.J.; Liu, Z.L.; Zou, L.; Yang, J. Influence of both friction and wear on the vibration of marine water lubricated rubber bearing. *Wear* **2017**, *376–377 Pt B*, 920–930. [[CrossRef](#)]
18. Tang, D.X.; Xiang, G.; Guo, J.; Cai, J.L.; Yang, T.Y.; Wang, J.X.; Han, Y.F. On the optimal design of staved water-lubricated bearings driven by tribo-dynamic mechanism. *Phys. Fluids* **2023**, *35*, 093611. [[CrossRef](#)]
19. Yang, T.Y.; Xiang, G.; Cai, J.L.; Wang, L.W.; Lin, X.; Wang, J.X.; Zhou, G.W. Five-DOF nonlinear tribo-dynamic analysis for coupled bearings during start-up. *Int. J. Mech. Sci.* **2024**, *269*, 109068. [[CrossRef](#)]
20. Liu, G.; Li, M. Lubrication characteristics of water-lubricated rubber bearings with partial wear. *J. Fluids Eng.* **2020**, *142*, 021209. [[CrossRef](#)]

21. Vaitkunaite, G.; Espejo, C.; Wang, C.; Thiebaut, B.; Charrin, C.; Neville, A.; Morina, A. MoS₂ tribofilm distribution from low viscosity lubricants and its effect on friction. *Tribol. Int.* **2020**, *151*, 106531. [[CrossRef](#)]
22. Mustafa, W.A.A.; Dassenoy, F.; Sarno, M.; Senatore, A. A review on potentials and challenges of nanolubricants as promising lubricants for electric vehicles. *Lubr. Sci.* **2021**, *34*, 1–29. [[CrossRef](#)]
23. Chen, Y.; Jha, S.; Raut, A.; Zhang, W.Y.; Liang, H. Performance characteristics of lubricants in electric and hybrid vehicles: A review of current and future needs. *Front. Mech. Eng.* **2020**, *6*, 571464. [[CrossRef](#)]
24. Deng, X.Q.; Wang, S.S.; Wang, S.K.; Wang, J.; Liu, Y.C.; Dou, Y.Q.; He, G.; Qian, L.M. Lubrication mechanism in gearbox of high-speed railway trains. *Tribol. Online* **2020**, *14*, JAMDSM0054. [[CrossRef](#)]
25. Zhang, S.; Jiang, S.; Lin, X. Static and dynamic characteristics of high-speed water-lubricated spiral-groove thrust bearing considering cavitating and centrifugal effects. *Tribol. Int.* **2020**, *145*, 106159. [[CrossRef](#)]
26. Will, F.; Boretti, A. A new method to warm up lubricating oil to improve the fuel efficiency during cold start. *SAE Int. J. Engines* **2011**, *4*, 175–187. [[CrossRef](#)]
27. Yan, B.; Dong, L.; Yan, K.; Chen, F.; Zhu, Y.S.; Wang, D.F. Effects of oil-air lubrication methods on the internal fluid flow and heat dissipation of high-speed ball bearings. *Mech. Syst. Signal Process.* **2021**, *151*, 107409. [[CrossRef](#)]
28. König, F.; Sous, C.; Jacobs, G. Numerical prediction of the frictional losses in sliding bearings during start-stop operation. *Friction* **2021**, *9*, 583–597. [[CrossRef](#)]
29. Fry, B.M.; Moody, G.; Spikes, H.A.; Wong, J.S.S. Adsorption of organic friction modifier additives. *Langmuir* **2020**, *36*, 1147–1155. [[CrossRef](#)]
30. Zhang, J.; Ueda, M.; Campen, S.; Spikes, H. Boundary friction of ZDDP tribofilms. *Tribol. Lett.* **2021**, *69*, 8. [[CrossRef](#)]

Disclaimer/Publisher’s Note: The statements, opinions and data contained in all publications are solely those of the individual author(s) and contributor(s) and not of MDPI and/or the editor(s). MDPI and/or the editor(s) disclaim responsibility for any injury to people or property resulting from any ideas, methods, instructions or products referred to in the content.